The Design of Barrel-Wound Foil Windings with Multiple Layers Interchanged to Balance Layer Currents

Jennifer D. Pollock, Charles R. Sullivan and Weyman Lundquist

jennifer.d.pollock@dartmouth.edu   charles.r.sullivan@dartmouth.edu   WLundquist@wcmagnetics.com

http://power.thayer.dartmouth.edu

Thayer School of Engineering

8000 Cummings Hall, Dartmouth College, Hanover, NH 03755, USA

Abstract— **This work investigates the performance of multi-layer foil windings in which the layers are interchanged to balance the flux linked by each layer and thus the current is shared equally between layers. Prototype transformers were built to confirm how much of the theoretical loss reduction is achievable in practice. The accuracy of the method to determine the location of the interchange is improved by considering individual turn lengths. In addition, the method is extended to any number of layers and several winding configurations. A discussion of the construction and termination of these windings is included as they greatly affect a component's performance.**

I. INTRODUCTION

FOIL windings are known for their low dc resistance compared to other winding types, but it is difficult to control the ac resistance at high frequencies. The ac resistance of a barrel-wound foil winding can rise rapidly with frequency. In order to reduce the high-frequency ac resistance both skin-effect and proximity-effect losses must be mitigated. Making the layer thickness (foil thickness) small compared to an electromagnetic skin depth can effectively reduce some components of high-frequency loss [1]. For a high-current winding, this requires connecting multiple layers of foil in parallel. However, each layer in the winding links a slightly different amount of flux. Because of the variation in flux linkage, the current does not split equally among the layers and tends to circulate in undesirable loops. Interchanging the layers can balance the flux between layers and reduce the imbalance and circulating losses [2]–[7]. This approach is similar to litz wire where individually insulated strands are twisted or woven together to cancel much of the flux that causes proximity-effect loss. Similar effects in parallel layers have also been studied in planar transformers [8], [9].

Using a foil winding instead of litz wire has the potential to improve packing factor to reduce winding resistance while also reducing cost. However, the approach taken to interchanging layer positions will have a substantial impact on cost. Using vias constructed with flexible printed-circuit board technology [2] is likely to be expensive. The approaches in [3] and [4] are likely to be less expensive, but experimental confirmation of high performance in a winding for a practical application has not previously been reported, and detailed design methods have been lacking.

This paper takes the approach introduced in [4], but develops more detailed, accurate and general design equations and verifies performance in a practical transformer. In this approach, interchanges of winding position are located along the length of the winding so that each turn links the same flux and therefore the current flows equally in each layer. The accuracy of the method to determine the location of the interchanges is improved by considering individual turn lengths. In addition, the method is extended to any number of layers and several winding configurations. An example transformer is designed for a 3.5 kW forward converter and prototypes have been built to verify the accuracy of the design method and the improvements in performance possible with interchanged, multi-layer barrel-wound foil windings.

TABLE I
TRANSFORMER SPECIFICATIONS

Parameter	Value	Units
Input Power	3.52	kW
Input voltage	350	V
Output voltage	52.5	V
Frequency	25	kHz
Turns Ratio	40T/6T	
Core Size	2 sets - E70/32/31	
Core Material	Epcos N87	

II. WINDING DESIGN THEORY

Consider a hypothetical single-turn single-layer foil winding, much thicker than an electromagnetic skin depth, with a sinusoidal current excitation, and with zero H field on one side and maximum H field on the other. It can,

in theory, be split into multiple thinner layers to reduce ac losses. If the current is made to share equally between p layers, the loss is reduced by a factor

$$\frac{P_{ml,opt}}{P_{sl}} = \frac{1.013}{\sqrt{p}} \tag{1}$$

where P_{sl} is the power loss in the thick single-layer winding and $P_{ml,opt}$ is the loss in the multi-layer winding if the foil height is chosen as [1]:

$$\frac{h_{foil,opt}}{\delta} = \frac{1.3}{\sqrt{p}} \tag{2}$$

where δ is the electromagnetic skin depth and $h_{foil,opt}$ is the optimal foil height for a given skin depth and number of layers.

More generally, for a multi-turn winding, the effective number of layers, p, is given by

$$p = \frac{N_t n_{l,t}}{f_w} \tag{3}$$

where N_t is the number of turns, $n_{l,t}$ is the number of layers per turn and f_w is a factor that reflects the electromagnetic configuration of the windings in the winding window. When the field is symmetric on both sides of the foil winding, as created by interleaving, f_w is 2. Because we will be comparing the performance of two foil winding designs with different foil thicknesses and numbers of layers, we will use

$$\frac{P_{p_a}}{P_{p_b}} = \frac{\sqrt{p_b}}{\sqrt{p_a}} \tag{4}$$

where $\frac{P_{p_a}}{P_{p_b}}$ is the ratio of the power loss in a design a to the power loss in design b and p_a is the number of layers in design a and p_b is the number of layers in design b to predict the improvement in performance of a winding configuration when both windings use the optimal thickness (2).

To realize performance approaching the theoretical loss reduction possible by dividing the foil into multiple parallel layers, we need to interchange the positions of those layers to achieve zero net flux in each loop defined by a pair of layers. One approach is to interchange them often enough that the net flux is likely to average out to be small. However, interchanging foil layers is more cumbersome than twisting wire, even with the relative simple approach in [4] of using pairs of slits halfway across the foil. Thus, we prefer a minimum set of necessary interchanges. In [4], these positions are calculated for a four-layer winding with the assumptions that the field is symmetric and the turn lengths are equal. To improve the precision of this calculation and allow addressing different numbers of layers, we present a more general calculation framework.

To achieve zero net flux between each pair of layers, we write the total flux between layers i and j, ϕ_{ij}, as

$$\phi_{ij} = \sum_{k=1}^{N_t} \phi_{ij,k} \tag{5}$$

where $\phi_{ij,k}$ is the flux between the layers in turn k,

$$\phi_{ij,k} = B_{ij,k} A_{ij,k} F_c \tag{6}$$

where $B_{ij,k}$ is the flux density between layers i and j for turn k, $A_{ij,k}$ is the area between the layers and F_c is a cross-over factor accounting for the direction that flux is linked. For layers before the position of an interchange, $F_c = +1$; for layers after the interchange $F_c = -1$ (to account for the reverse linkage of the flux); and for layers containing an interchange,

$$F_c = 1 - 2\frac{\ell_x}{\ell_k} \tag{7}$$

where ℓ_k is the length of turn k and ℓ_x is the distance from the start of the turn to the interchange. The area between two layers for one turn is

$$A_{ij,k} = \ell_k t_{insulation} \tag{8}$$

where $t_{insulation}$ is the thickness of the insulation between layers. We have chosen to assume that the length of a turn is constant for all areas between layers in that turn. The flux density between two layers for one turn is

$$B_{ij,k} = B_{peak}\frac{m}{p} \tag{9}$$

where the m is the index of the position of the space between the layers under consideration counting from a point of zero flux density. The value of m depends on the electromagnetic field configuration, the number of layers per turn and the number of turns. A value for peak flux density in the winding window is not needed for calculating interchange positions, but if it is needed for other purposes it may be approximated by

$$B_{peak} = \frac{N_t I_{peak}}{b_{window}}\mu_0 \tag{10}$$

where I_{peak} is the peak current in the winding, b_{window} is the breadth of the winding window (see Fig. 3), and μ_0 is the permeability of free space.

Given the formulation of net flux in (5), the position of an interchange that results in zero net flux is

$$\ell_x = \frac{(\sum_{k=1}^{k_x-1} m_k\ell_k) + (\sum_{k=k_x+1}^{N_t} -m_k\ell_k) + m_{k_x}\ell_{k_x}}{2m_{k_x}} \tag{11}$$

where k is the index number of a turn, ℓ_k is the length of turn k, k_x is the turn with the interchange in it, m_k is the

index of the space between the layers under consideration in turn k counting from a point of zero flux density. We can construct a vector m from the values of m_k for each value of k for each pair of layers, i and j. The vector m is developed for several examples in the next section.

TABLE II
DETAILS OF EXAMPLE CONFIGURATIONS

Example	A	B	C
Interchanges	1	2	4
$n_{l,t}$	2	4	8
f_w	1	2	2
p	12	12	24
Reduction in power loss $(1 - \frac{P_{n_{l,t}}}{P_{sl,t}})$	70.7%	50%	12.5%

TABLE III
POSITION INDEX, m, FOR EXAMPLE CONFIGURATIONS WHERE k IS THE TURN NUMBER.

Example	i,j	$k=1$	$k=2$	$k=3$	$k=4$	$k=5$	$k=6$
A	1,2	1	2	3	4	5	6
B	1,2	9	5	1	-1	-5	-9
B	2,3	10	6	2	-2	-6	-10
B	3,4	11	7	3	-3	-7	-11
C	1,2	22*	-13	-5	3	11	19
C	{1,2},{3,4}	22	-14	-6	2	10	18
C	3,4	22*	-15	-7	1	9	17
C	{1234,5678}	20	12	4	-4	-12	-20
C	5,6	19	11	3	-5	-12	-22*
C	{5,6},{7,8}	18	10	2	-6	-14	-22
C	7,8	17	9	1	-7	-15	-22*

* indicates a value found by simple averaging where ideally a weighted average would be used. See text.

A. Example Designs

We have chosen to consider several designs with one interchange, two interchanges and four interchanges for the transformer described in Table I. Because each interchange increases the complexity of construction, we wanted to examine configurations with the smallest number of interchanges that can offer a substantial reduction is loss if the current can be made to split equally among the layers. Table III shows the vector m for the three different example configurations. For certain winding configurations, for example when there are four layers per turn and the field is not symmetric, the formulation of the m vectors is more complicated.

The configuration of Example A is detailed in Table II and has two layers per turn and an asymmetric field that rises from zero on one side to a maximum on the other side. The electromagnetic factor, f_w, is one for an asymmetric
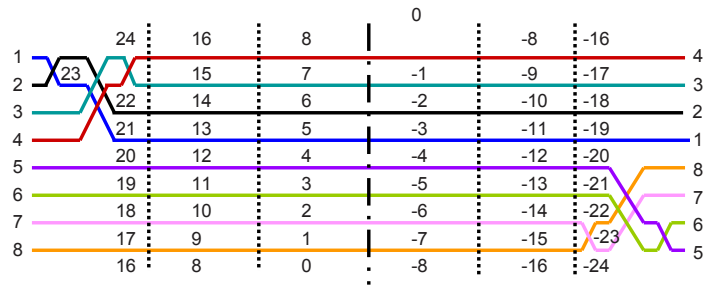

Fig. 1. An eight-layer interchanged winding shown before being wound to demonstrate how to build the m vectors for a more complicated design. The vertical lines delineate the six turns and the numbers in the spaces between the layers are the value of m for that position starting from the point of zero flux.

field configuration and thus the effective number of layers, p, is twelve as listed in Table II. The theoretical reduction in loss is predicted to be 29% based on (4). Because this design has only two layers, there is only one m vector and it is shown in Table III.

Example B is that of the constructed prototypes, with 4 layers per turn and a symmetric field configuration. This configuration has two interchanges and three m vectors, one for each set of layers, $i,j = \{1,2\}, \{2,3\}$, and $\{3,4\}$. The theoretical reduction in loss is predicted to be 50% based on (4). The number of effective layers, p, is found with (3) and is equal to 3 when $n_{l,t}$ is 1 and 12 when $n_{l,t}$ is 4.

Example C has 8 layers per turn and a symmetric field configuration, thus the number of effective layers, p, is 24. This winding requires four interchanges, but the predicted loss reduction is 87% so the complexity of construction maybe justified when efficiency is a driving design parameter. The m vectors for this design, given in Table III, can be found by examining Fig. 1 which shows the eight-layer, six turn winding unwound, but with the interchanges shown and the field strength indices m indicated in each interlayer space. Asterisks in Table III indicate values that are averages of two different values because a higher-level interchange involving the layers in question occurs within a layer. Most properly, this would be a weighted average based on the position of the other interchange. However, precise calculation of the weighted average is not important because the values being averaged are very similar: in this example, the weighted averages are between 21 and 23, and we ignore the weighting and use 22 as the average.

III. TRANSFORMER DESIGN, PROTOTYPE CONSTRUCTION AND MEASUREMENT

A transformer was designed for a 3.5 kW forward converter as specified in Table I using the design method in [4] which has been improved and detailed in Section II.

Fig. 2. Four-layer, interchanged foil winding prototype. The terminations of the secondary are on the right and the primary leads on the left.

TABLE IV

COMPARISON OF FOIL WINDING PERFORMANCE AT 25 KHZ

Parameter	Single Layer	Four Layers
Number of Layers	1	4
Optimal Foil Height, $h_{foil,opt.}$, mm	0.32	0.16
Actual Foil Height, $h_{foil,act.}$, mm	0.69	0.18
$\frac{h_{foil,opt}}{\delta}$	0.75	0.37
Calc. $R_{dc,s}$, mΩ with $h_{foil,act.}$	0.85	0.82
Measured $R_{dc,s}$, mΩ	1.030	1.065
Calc. $R_{ac,s}$ by Dowell's method, mΩ	3.0	1.1
Measured $R_{ac,s}$, mΩ	6.0	3.0
2D FEA XY model $R_{ac,s}$, mΩ	5.8	NA

The primary winding of the transformer was interleaved around the secondary as shown in Fig. 3. Interleaving the windings as shown provides a reduction in loss by reducing the peak field in the winding window without excessively increasing the complexity of construction. The secondary winding has six turns, as shown in Fig. 3. We consider a single-layer design, where the number of layers per turn, $n_{l,t}$ is 1 and a four-layer design where $n_{l,t}$ is 4. According to (1), increasing the number of layers from one to four could theoretically reduce losses by 50%.

Eq. (2) was used to find that the optimal foil thickness for a single-layer foil winding is 0.32 mm thickness and that the optimal foil thickness for a four-layer, interleaved foil winding is 0.16 mm thickness. We chose to make the single-layer foil winding with a foil thickness 0.69 mm in order to have essentially the same cross-sectional area as the four-layer winding, and thus the same dc resistance. The interchange locations for the four-layer winding were determined to be at $\ell_1 = 58.4$ mm and $\ell_2 = 1231.4$ mm from the start of the winding. The start of the winding is defined as the location where all layers are connected across the width of the foil as shown in Fig. 5.

Prototypes were constructed with the same primary wind-

ing design and different secondary winding designs. The four-layer, interchanged prototype is shown in Fig. 2. The primary is composed of 480/44 (number of strands/AWG) litz wire and sections of the primary winding were connected in series. Very fine strands (AWG 44) were used to ensure that the ratio of ac to dc resistance, F_r, would be approximately equal to 1 and thus the ac resistance of the primary would be equal to the dc resistance. We used the loss calculation detailed in [10] where the winding loss is

$$P_{loss} = F_r I_{ac,rms}^2 R_{dc} \qquad (12)$$

where $I_{ac,rms}$ is the rms value of the as current in a winding and R_{dc} is the dc resistance. F_r is given as

$$F_r = 1 + \frac{\pi^2 \omega^2 N^2 n^2 d_c^2 k}{768 \rho_c b_c^2} \qquad (13)$$

where ω is the angular frequency, N is the number of turns, n is the number of strands, d_c is the diameter of the strand, k is a factor for the field distribution is multi-winding transformers (see [10]), ρ_c is the resistivity of conductor and b_c is the breadth of the winding window. For the primary of the prototype transformer, $F_{r,p}$ was calculated to be 1.00002 using (13).

The dc resistance of each winding was measured with an Agilent 34420A micro-ohm meter. Table IV compares the calculated and measured dc resistances for the foil secondaries and shows that the measured dc resistance was only slightly higher than the predicted dc resistance. This confirms that neither the leads or the notches contribute excessively to the dc resistance. The measured dc resistance of the single-layer and four-layer windings are essentially equal as they were designed to be.

The ac resistance of the secondary was measured using an Agilent 4294A impedance analyzer with the split primary connected in series and shorted. All windings were measured with the same core. The ac resistance of the primary was determined from the measured dc resistance and the calculated ratio of ac to dc resistance, $F_{r,p}$, and was removed from the measured ac resistance to find the measured ac resistance of the secondary

$$R_{ac,s} = R_{ac,measured} - \left(\frac{N_s}{N_p}\right)^2 F_{r,p} R_{dc,p} \qquad (14)$$

where $R_{ac,measured}$ is the ac resistance measured at the secondary with the primary connected in series and shorted, and $R_{dc,p}$ is the measured dc resistance of the primary. It should be noted that using $F_{r,p} = 1$ is the smallest resistance that can be subtracted from the measured resistance. If F_r were greater than one, the calculated performance of the secondary would improve because the ac resistance would

be lower. For each prototype, the measured ac resistance of the secondary given by (14) is shown in Fig. 6.
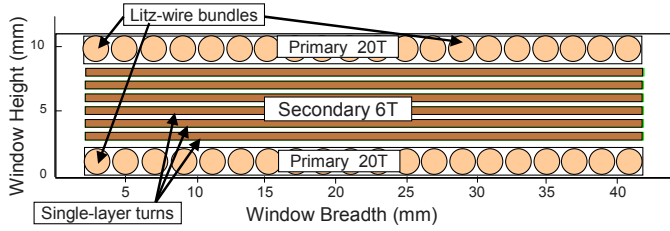

Fig. 3. The location of the windings in the winding window. The primary winding is split in half and wound around a foil secondary. The cross-section shows the single-layer design for the foil secondary, where the number of turns. $N_t = 6$ and the number of layers per turn, $n_{l,t} = 1$. Each section of the primary has 20 turns, each a bundle of litz wire composed of 480 strands of AWG 44.)

IV. DISCUSSION OF RESULTS

The measured ac resistance of the four-layer, interchanged foil winding was 50% lower than the measured ac resistance of a single-layer design at 25 kHz as shown in Fig. 6. The reduction in ac resistance is approaching the 63% predicted by Dowell's method [11], and is substantial enough to make the increased complexity of construction worthwhile. Interchanging the layers of a multi-layer, multi-turn foil winding is an effective strategy for reducing winding resistance.

Fig. 7 shows the ac resistance of the single-layer design based on measurement, Dowell's method [11], and by two-dimensional (2D) and three-dimensional (3D) finite element analysis (FEA). For the single-layer foil winding, the measured ac resistance matches the 2D FEA model within 3.5% at the design frequency. In addition, the ac resistance predicted by the 2D FEA model follows the shape of the measured ac resistance curve over a large frequency range. A large amount of computing resources is necessary to solve a three-dimensional model of this complexity to the desired degree of accuracy. The 3D FEA results shown in Fig. 7 for the single-layer design were solved to within 1% energy error compared to the 2D model which was solved to within 0.001% energy error. We expected the ac resistance predicted by Dowell's method to underestimate the measured ac resistance because the calculation considers only a one-dimension field and does not include edge effects or terminations.

A. Terminations

Because the method presented here accounts for flux between layers, any extra area available to capture flux
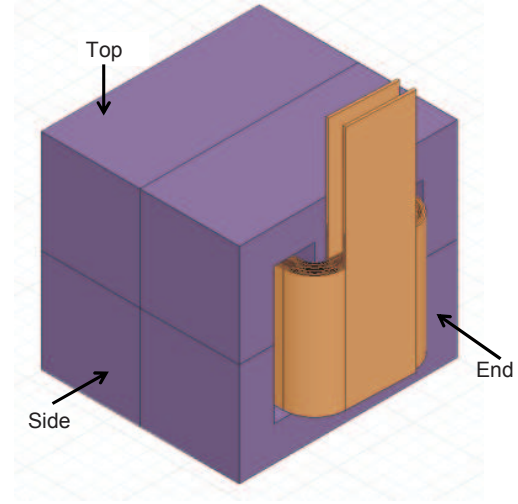

Fig. 4. A 3D model of the single-layer prototype used for finite element analysis and shows only the secondary foil winding. The figure shows the top, side and end view of the component referenced in Fig. 5.
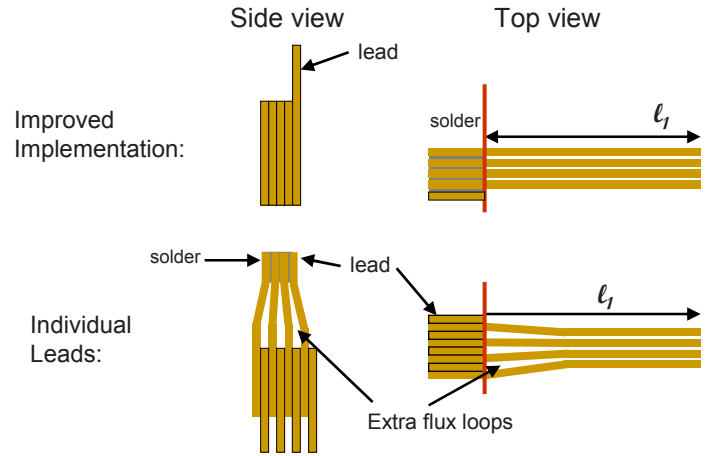

Fig. 5. The terminations of a multilayer, interleaved foil winding must be constructed so each layer starts at the same location to ensure equal current sharing. Please refer to Fig. 4 for the orientation of the views.

would degrade the performance. We built some prototypes with a lead connected to each layer in the winding and found that they did not preform as predicted. The leads were similar to the configuration shown in the bottom of Fig. 5 where the leads were thicker than the foil used in the winding. This created extra area between the layers that were not accounted for in the design of the winding. In addition, there was not a clearly defined starting point for the winding, from which to measure the distance to the first interchange. The start of the winding should ideally be the point at which it splits into multiple layers.

Proper terminations were key to the performance of the prototype windings reported here. The top sketch in Fig. 5 shows terminations used the prototypes presented in this
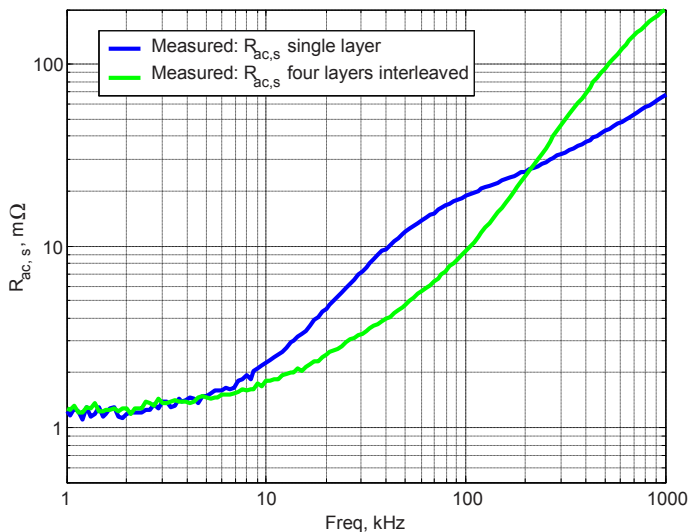
Fig. 6. The measured ac resistance of a four-layer, interleaved foil winding is compared to the measured ac resistance of the single layer design.
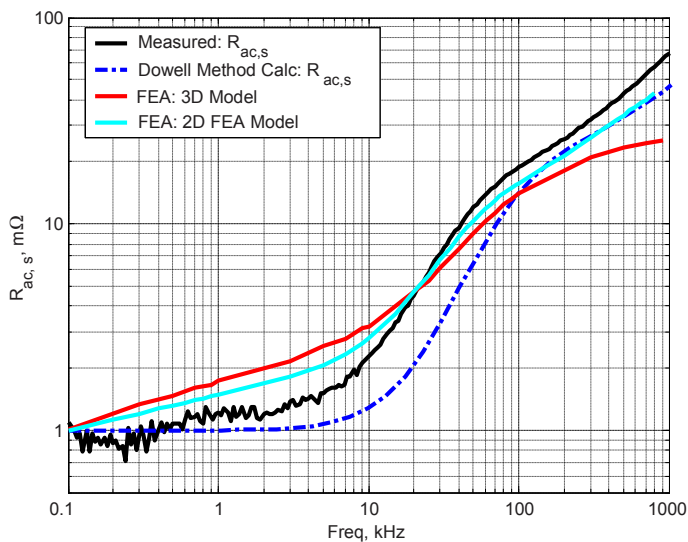

Fig. 7. The measured ac resistance of single-layer winding is compared to the ac resistance predicted by Dowell's method, 2D FEA and 3D FEA.

work. All the layers were soldered together across the entire width of the winding and then one lead was soldered to that connection to exit the winding as shown in Fig. 2. This termination structure minimized any extra flux loops and the winding performed as predicted.

V. CONCLUSION

Multi-layer, barrel-wound foil windings with layers interchanged to balance flux can be used to reduce the ac resistance of foil windings in transformers. In this work, we have shown that a 50% reduction in ac resistance is possible

through the use of interchanged, multi-layer windings while maintaining the same dc resistance. This reduction in ac resistance was achieved in part by proper construction of the winding terminations. The foil winding configurations used here have demonstrated the energy savings possible in high-power, high-frequency transformers used in isolated power converters.

REFERENCES

[1] M. E. Dale and C. R. Sullivan, "General comparison of power loss in single-layer and multi-layer windings," in *36th Annual IEEE Power Electronics Specialists Conference*, 2005.
[2] W. O. J. v. W. S. Wang, M. de Rooij and D.Boroyevich, "Reduction of high-frequency conduction losses using a planar litz structure," in *IEEE Transactions on Power Electronics*, vol. 20, no. 2, 2005.
[3] J. S. Glaser and M. A. de Rooij, "A novel folded litz ribbon cable for magnetic components," in *IEEE Power Electronics Specialists Conference*, 2007.
[4] M. Nigam and C. R. Sullivan, "Multi-layer barrel-wound foil winding design," in *IEEE XXnd Annual Power Electronics Specialists Conference*, 2008, pp. 1–6.
[5] Y. Y. B. B. X. Dexin, Y. Xiuke and N. Takahashi, "Circulating current computation and transposition design for large current winding of transformer with multi-section strategy and hybrid optimal method," in *IEEE Transaction on Magnetics*, vol. 36, no. 4, 2000, pp. 1014–1017.
[6] C. J. B. Baodong, X. Dexin and F. Zhenyao, "Optimal transportation design of transformer windings by genetic algorithms," in *IEEE Transaction on Magnetics*, vol. 31, no. 6, 1995, pp. 3572–3574.
[7] S. Kulkarni and S. Kharparde, "Stray loss evaluation in power transformers-a review," in *IEEE Power Engineering Society Winter Meeting*, 2000.
[8] J.-P. K. A. B. X. Margueron, "Current sharing between parallel turns of a planar transformer: Prediction and improvement using a circuit simulation software," in *IEEE Industry Applications Society Meeting*, 2007.
[9] Y. H. Wei Chen, Yipeng Yan and Q. Lu, "Model and design of pcb parallel winding for planar transformer," in *IEEE Transaction on Magnetics*, vol. 39, no. 5, 2003, pp. 3202–3204.
[10] C. R. Sullivan, "Optimal choice for number of strands in a litz-wire transformer winding," *IEEE Transactions on Power Electronics*, vol. 14, no. 2, pp. 283–291, 1999.
[11] P. Dowell, "Effects of eddy currents in transformer windings," *Proceedings of the IEE*, vol. 113, no. 8, pp. 1387–1394, Aug. 1966.